Deformation behaviour of intersecting tunnels

by Vaishali Narula

Submission date: 15-Jun-2026 03:29PM (UTC+0530)
Submission ID: 2983628375
File name: Major_Project_Report__Vaishali_Narula_1_1_z_2.pdf (4.36M)
Word count: 6614
Character count: 39306

CHAPTER 1

INTRODUCTION

1.1 General

Underground construction has become an essential component of modern infrastructure development due to increasing urbanization, limited surface space, and the growing demand for efficient transportation systems. Tunnels are widely used for highways, railways, metro systems, water conveyance, and utility corridors. With the expansion of such infrastructure, the requirement for multiple underground openings in close proximity has increased significantly. As a result, the construction of intersecting or closely spaced tunnels has become increasingly common in both urban and mountainous regions.

Tunnel intersections are often unavoidable in complex projects such as multi-level transportation networks, underground interchanges, and diversion systems. However, the presence of an additional tunnel in the vicinity of an existing one alters the in-situ stress conditions of the surrounding rock mass. This interaction leads to redistribution of stresses, which in turn causes deformation and potential instability in the tunnel system. Therefore, understanding the deformation behaviour of intersecting tunnels is of critical importance for ensuring safety, serviceability, and long-term performance.

1.2 Background of the Study

The behaviour of a single tunnel under static loading conditions has been extensively studied in rock mechanics and geotechnical engineering. However, when two tunnels intersect or are constructed in close proximity, the problem becomes more complex due to interaction effects. The excavation of a new tunnel induces additional stress changes in the rock mass surrounding the existing tunnel, which may result in increased deformation, cracking, or even structural failure if not properly accounted for.

In practical scenarios, tunnel intersections may occur at various angles and distances, further complicating the stress distribution patterns. Among these, oblique intersections (such as 30°) are particularly critical because they produce non-uniform stress concentrations and asymmetric

deformation patterns. The intersection zone, especially the crown region, is often identified as the most vulnerable location due to stress concentration and reduced confinement.

Despite the availability of advanced numerical tools, there is still a need for experimental validation to ensure the reliability of predicted results. Physical modelling provides valuable insights into deformation behaviour and helps in understanding complex interaction mechanisms that may not be fully captured through numerical simulations alone.

1.3 Problem Statement

The design and analysis of a scaled-down physical tunnel model and numerical analysis to simulate the behaviour of an actual proposed intersecting Chenani-Nashri tunnel in Himalayan region. This is to predict the deformation at the various critical sections of the tunnel such as portal, crown and invert. However significant discrepancies exists between numerical analysis and physical modeling. The Himalayan geology is characterized by weak rock formations and high in-situ stresses. Tunnel intersections in such geological environments are particularly vulnerable to excessive deformation and stress concentration. Most existing studies focus primarily on numerical analysis, with limited emphasis on experimental validation. Numerical analysis and experimental investigations using Piezoelectric Lead Zirconate Titanate (PZT) sensor-based monitoring were carried out under static loading conditions. Therefore, there is a need for a comprehensive study that combines numerical modelling with experimental investigation to accurately assess the deformation behaviour of intersecting tunnels.

1.4 Objectives of the Study

The primary aim of this study is to investigate the deformation characteristics of intersecting tunnels under static loading conditions. The specific objectives are as follows:

- To analyse the deformation behaviour of tunnel intersections using 3D numerical analysis software
- To develop a scaled physical model representing intersecting tunnels
- To measure deformation at critical locations (Portals, Crown and Invert) using piezoelectric sensors

- To validate numerical results with experimental observations
- To identify the most critical zones of deformation within the tunnel system

1.5 Scope of the Study

This study focuses on both numerical and experimental analysis of tunnel intersection behaviour under controlled static loading conditions. The scope includes:

- Three-dimensional numerical modelling using the Hoek–Brown failure criterion
- Simulation of realistic rock mass properties based on a case study (Chenani–Nashri tunnel)
- Laboratory-scale physical modelling using Plaster of Paris
- Measurement of deformation using PZT sensors
- Comparative analysis of numerical and experimental results

However, the study is limited to static loading conditions and does not consider dynamic effects such as seismic loading or blasting vibrations.

CHAPTER 2. LITERATURE REVIEW

2.1 Rock mass behaviour and failure criteria

The mechanical behaviour of rock masses surrounding tunnels plays a critical role in determining deformation characteristics. Unlike intact rock, rock masses are inherently discontinuous due to the presence of joints, fractures, and bedding planes. As a result, their behaviour is nonlinear and often anisotropic.

One of the most widely used criteria for modelling rock mass behaviour is the **Hoek**–Brown failure criterion, introduced by Hoek and Brown (1980) and later refined in 2002 [1,2]. This criterion accounts for the nonlinear strength characteristics of jointed rock masses and is particularly suitable for underground excavation problems. It incorporates parameters such as the Geological Strength Index (GSI), intact rock strength, and material constants to represent real field conditions.

Several studies have demonstrated that the Hoek–Brown model provides more realistic predictions of deformation and failure compared to traditional linear models such as Mohr–Coulomb, especially for highly fractured rock masses [3].

2.2 Deformation behaviour of Single tunnel

The deformation behaviour of a single tunnel has been studied extensively using both analytical and numerical approaches. When a tunnel is excavated, the in-situ stress field is disturbed, leading to stress redistribution around the opening. This results in radial displacement (convergence) and tangential stress concentration, particularly at the crown and sidewalls.

Wang and Yin (2010) developed analytical solutions for circular tunnels in elastic–plastic media, showing that deformation is highly dependent on rock mass properties and in-situ stress conditions [4]. Similarly, numerous numerical studies using finite element and finite difference methods have highlighted that maximum deformation typically occurs at the crown region due to stress concentration.

Similarly, Oreste(2003) introduced the convergence–confinement method, which describes the relationship between ground reaction and tunnel support [5]. This approach has been widely used to understand tunnel deformation and support interaction.

However, these studies are primarily limited to isolated tunnels and do not account for interaction effects caused by nearby excavations.

2.3 Interaction of twin tunnels

The interaction between closely spaced tunnels has been a subject of increasing research interest. When two tunnels are excavated near each other, the stress field around one tunnel influences the other, resulting in complex deformation patterns.

Ng et al. (2004) conducted numerical studies on twin parallel tunnels and observed that the deformation of each tunnel increases significantly as the spacing between them decreases. It also investigated the behaviour of closely spaced tunnels in soft ground and observed that the second tunnel excavation induces additional settlement and deformation in the first tunnel [6]. The study concluded that interaction effects become critical when the spacing is less than two to three times the tunnel diameter. These findings emphasize the importance of considering tunnel interaction during design.

Similarly, Li et al. (2016) investigated the deformation behaviour of twin tunnels and found that stress superposition leads to increased displacement at the sidewalls and crown regions [7]. The study emphasized the importance of considering tunnel interaction during the design phase to avoid structural instability.

These studies highlight that tunnel spacing, depth, and sequence of excavation are key parameters influencing deformation behaviour.

2.4 Behaviour of Intersecting Tunnels

Intersecting tunnels represent a more complex case compared to parallel tunnels due to their three-dimensional geometry and varying intersection angles. When a new tunnel intersects an

existing one, the stress field becomes highly non-uniform, leading to localized deformation and potential instability.

Studies have shown that the intersection zone is the most critical region, where stress concentration and deformation are significantly higher than in other parts of the tunnel. In particular, the crown region at the intersection experiences maximum displacement due to reduced confinement and stress redistribution.

Research by Zheng et al. (2020) on intersecting tunnels demonstrated that the angle of intersection plays a significant role in determining deformation patterns [8]. Smaller intersection angles (e.g., 30°–45°) result in asymmetric stress distribution and higher deformation compared to perpendicular intersections.

Liu et al. (2017) used numerical modelling to study the stability of intersecting tunnels and found that the presence of a new tunnel can increase deformation in the existing tunnel by up to 50%, depending on the spacing and depth [9].

Compared to parallel tunnels, intersecting tunnels present a more complex problem due to the three-dimensional nature of stress redistribution. When a new tunnel intersects an existing one, the stress concentration becomes highly localized at the intersection region, leading to significant deformation.

Research indicates that the intersection crown is the most critical location, as it experiences maximum stress concentration and deformation. Oblique intersections, such as those at angles less than 90°, produce asymmetric stress distribution, making the analysis more challenging.

2.5 Stresses around underground tunnels

This is a major parameter in designing the underground structures. Evaluation of stresses and displacement around the circular opening becomes important. There are various methods to determine the stress distribution around the circular opening and researchers had also given their theories and solutions for stresses acting around underground structures. Kirsch analytical method for stress around circular opening in plain strain condition given in1898 is [10] :

$$\sigma_r = 1/2(\sigma_x + \sigma_z)(1 - a^2/r^2) + 1/2(\sigma_x - \sigma_z)(1 - 3a^4/r^4 - 4a^2/r^2)\cos 2\theta \quad (1)$$

$$\sigma_\theta = 1/2(\sigma_x + \sigma_z)(1 + a^2/r^2) - 1/2(\sigma_x - \sigma_z)(1 + 3a^4/r^4)\cos 2\theta \quad (2)$$

$$\tau_{r\theta} = -1/2(\sigma_x - \sigma_z)(1 - 3a^4/r^4 + 2a^2/r^2)\sin 2\theta \quad (3)$$

σ_r = radial normal stress

σ_θ = tangential normal stress

$\tau_{r\theta}$ = shear stress

$\sigma_z = \gamma h$ = overburden pressure

$\sigma_x = K\sigma_z$ = horizontal pressure

where, a = radius of the opening; r = radial distance from the centre of opening

Several studies have employed three-dimensional numerical modeling to investigate the mechanical behavior of tunnel intersections and closely spaced tunnels under varying geological and loading conditions. Chortis and Kavvadas (2020) conducted 3D numerical analyses on perpendicular tunnel intersections and demonstrated that such intersections significantly alter stress distributions in the surrounding rock mass and primary support system [11]. Their results indicated additional compressive loading at the spring line of the main tunnel, while the crown and invert may experience either compressive loading or unloading, occasionally reaching tensile states. However, the study was limited by the absence of validation using real project data and a restricted range of intersection geometries. Similarly, Chehade and Shahrour (2008) investigated the interaction between twin tunnels and reported that interaction effects decrease with increasing center-to-center spacing, becoming minimal for spacing-to-diameter ratios (S/D) greater than or equal to three, whereas significant interaction occurs for S/D ratios below two

[12]. Despite these insights, the study lacked real-time construction data and did not fully address complex geological conditions.

2.6 Research Gap

Based on the review of existing literature, the following gaps have been identified:

- Limited studies on intersecting tunnels under static loading conditions
- Lack of combined numerical and experimental validation
- Insufficient data on deformation at specific locations (crown, invert, portals)
- Need for studies incorporating realistic rock mass parameters from actual projects

The literature indicates that tunnel interaction significantly influences deformation behaviour, particularly at the intersection region. While numerical methods provide valuable insights, experimental validation is essential for accurate prediction.

The present study addresses these gaps by combining 3D numerical modelling using MIDAS GTS NX with experimental investigation using PZT sensors, thereby providing a comprehensive understanding of deformation behaviour in intersecting tunnels.

CHAPTER 3. METHODOLOGY

3.1 Numerical Modelling

Advancements in computational tools have enabled detailed analysis of complex underground structures. Software such as MIDAS GTS NX, FLAC3D, and PLAXIS 3D are commonly used for tunnel analysis.

MIDAS GTS NX, in particular, provides a robust platform for three-dimensional modelling of geotechnical problems. It supports advanced material models such as Hoek–Brown and allows simulation of realistic boundary conditions.

Numerical modelling offers several advantages:

- Ability to simulate complex geometries
- Flexibility in changing parameters
- Visualization of stress and deformation contours

However, numerical models require validation through experimental or field data to ensure reliability.

3.1.1 Model Geomtery

A three-dimensional numerical model was developed using 3D Numerical analysis software to simulate the existing tunnel and a newly proposed intersecting tunnel. The model was designed to replicate realistic field conditions by incorporating rock mass properties derived from the Chenani–Nashri tunnel project. 3D modeling is preferred over 2D model because excavation sequence simulation is possible in 3D and also relaxation calculation is not required in 3D modeling.The Hoek–Brown failure criterion was used to represent the nonlinear behaviour of the rock mass, which is suitable for jointed geological formations.

The numerical model consists of existing circular tunnel and an escape tunnel. The new proposed tunnel intersecting existing escape tunnel at an angle of 30°. But for the purpose of ease of calculation the diameter of escape tunnel and existing tunnel is taken same. The diameter of the

prototype tunnel is 8.5 m. The new tunnel intersects the existing tunnel at a specified distance from the portal, replicating the experimental configuration.

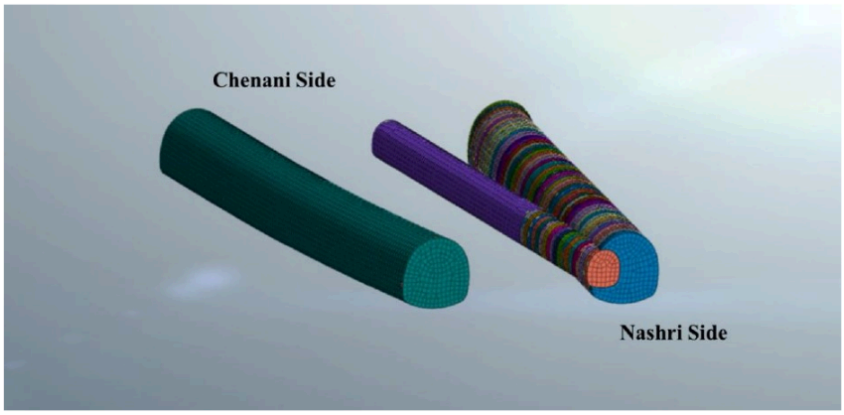

Fig 1 . Model Geometry of tunnel intersection from Nashri Side

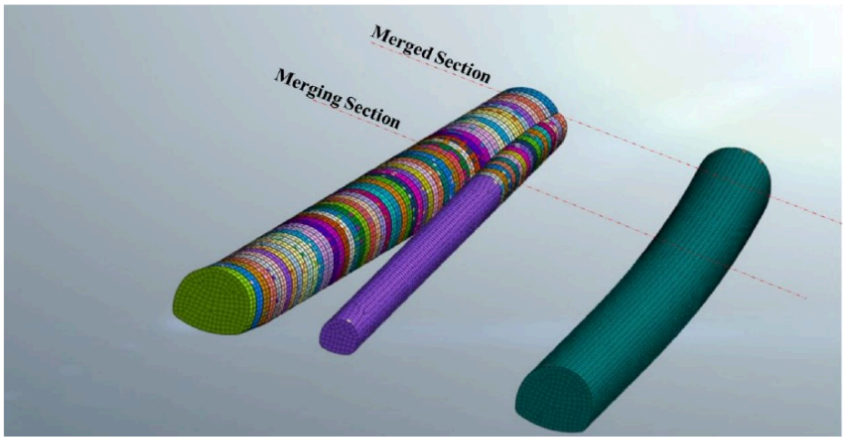

Fig 2 . Model Geometry of tunnel intersection from Chenani Side

3.1.2 Material Properties

Rock mass properties used in the numerical model were based on real project data to ensure practical relevance. The Hoek–Brown parameters were derived using Geological Strength Index (GSI), uniaxial compressive strength (UCS), and deformation modulus.

Table I. Rock mass properties along the proposed tunnel length at the Project site (Source: *Detailed Project Report- Dr. Shyama Prasad Mukherjee Tunnel)*

Rock class	RMR	GSI	UCS	Overburden	Mi	Mr	Mb	S	A	Erm
A2	70	65	100	700	17	275	4.231	0.0155	0.502	14046.9
B1	60	55	110	1030	17	325	3.408	0.00673	0.504	14596
B2	55	50	80	600	17	325	2.851	0.00386	0.5057	7986.8
B3	50	45	70	400	17	325	2.384	0.0022	0.5081	5088
C1	35	30	50	100	17	375	1.395	0.00041	0.5223	1525.93
C2	35	30	40	300	10	300	0.821	0.00041	0.5223	976.6
C3	40	35	65	720	10	325	0.981	0.00073	0.5159	3399.8
C4	40	35	35	500	10	325	0.981	0.00073	0.5159	2494.8

At the intersection the rock mass class is C2, hence the properties and values of C2 type rock mass is taken into consideration for design of tunnel intersection. Poisson's ratio of 0.2 and deformation modulus of 1000-14000 MPa is taken as a input values.

3.1.3 Boundary conditions and Loading

The boundary conditions for the numerical model were carefully defined to realistically represent the in-situ confinement and support conditions of the ground mass while minimizing boundary-induced effects on the analysis results. Appropriate constraints were assigned to different model boundaries to ensure numerical stability and to simulate the actual field response of the rock system under loading conditions.

The model boundaries were defined to simulate in-situ constraints:

- Bottom boundary: Fully fixed. In this condition, all translational degrees of freedom were restrained, preventing displacement in both horizontal and vertical directions [13]. This assumption represents the presence of a sufficiently stiff underlying stratum at depth, which restricts movement beneath the analysed domain. Fixing the base also prevents rigid body motion of the model during analysis and ensures stability of the finite element solution.

- Side boundaries: Roller support (restrict horizontal displacement). The vertical side boundaries were modelled using roller supports, where horizontal displacement was restricted while vertical movement was permitted [14]. This boundary condition simulates the continuity of the surrounding ground beyond the model extent and allows settlement to occur naturally under loading without introducing excessive lateral deformation. By restricting only the horizontal movement, the side boundaries approximate field conditions where the adjacent soil mass provides lateral confinement to the analysed section.

- Top surface: Free. The top surface of the model was kept free of constraints, allowing unrestricted deformation in response to the applied loads [15]. This condition reflects the actual ground surface behaviour where vertical settlement and minor lateral deformation may occur due to external loading. Maintaining a free upper boundary enables the model to capture realistic stress distribution and displacement patterns near the surface.

Static loading conditions were applied to simulate overburden pressure.

3.1.4 Meshing and Analysis

A three-dimensional finite element mesh was generated to discretize the model domain. Finer mesh elements were used near the tunnel intersection region to capture stress concentration and deformation accurately.

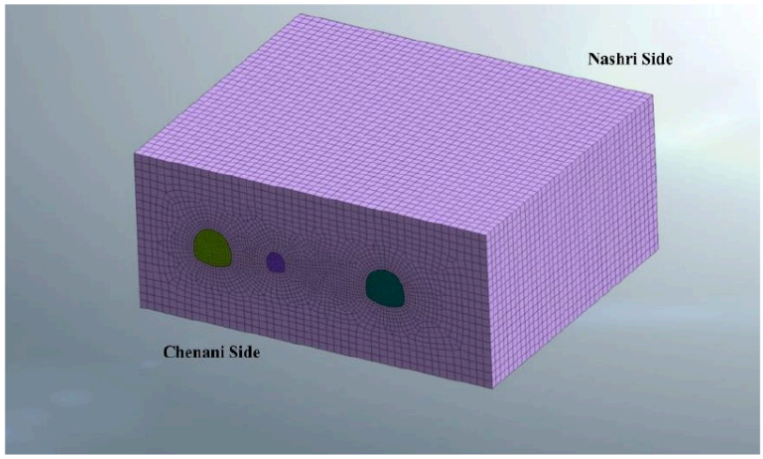

Fig 3. Meshing of tunnel intersection model from Chenani side

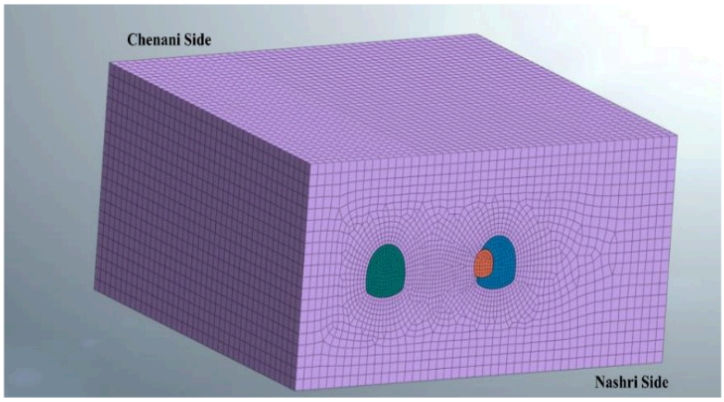

Fig 4. Meshing of tunnel intersection model from Nashri side

The analysis was carried out in stages to simulate excavation and loading conditions.

3.2 Experimental Modelling in Tunnel studies

3.2.1 Rock condition in Himalayan Region

Figure 5. Project Site Location of Chenani Nashri Tunnel (Source: BHUVAN)

The study area lies in outer, lesser and Tethyan Himalayan region consisting of Shivaliks, murrees, and pre tertiary sediments, karewas and sirban group. These sediments constitute sandstone, shales, conglomerates and clay beds. The proposed tunnel alignment is as follows:

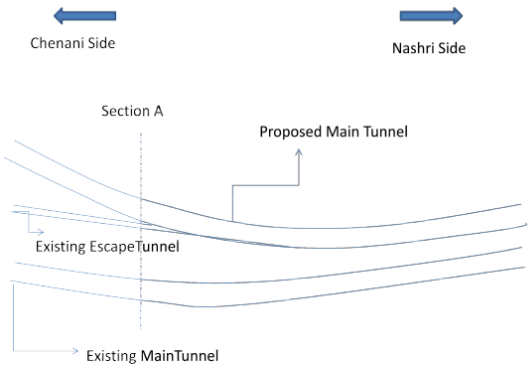

Fig 6. Schematic View of the Chenani Nashri tunnel

3.2.2 Similarity Analysis

a) Geometric Similarity:

$\lambda_{L=}D_P / D_m$; D_p= diameter of prototype =13m and D_m= diameter of model

Let the scale be λ_L= 1:256 ➔ 1/256 = 13/ D_m ➔ D_m = 0.05m = 50mm

Prototype length considered for the analysis = 110m ; so Model length = 110m x λ_L= 425mm

b) Density Scaling:

λ_ρ = Density of model/ density of prototype = 730/ 2600= 1/3.56 = 0.0281

c) Stress Scaling:

$\lambda_{\sigma =} \lambda_\rho$ x λ_L = 0.0281 x 0.00391 = 0.0011 = 1/909

d)Elastic modulus scale:

$\lambda_{E =} E_m$ / Ep = 3000/ 976.6 = 3.07

e) Load Scale:

$\lambda_P=\lambda_\sigma$ x λ_L^2 = 0.0011 x $(0.00391)^2$ = 1.68 x 10^{-8}

f) Rock modulus ratio:

Young's modulus of lining/ Young's modulus of rock = 28000 / 976.6= 28.67

While, prototype rock mass modulus/ model material modulus= E_p/ E_m = 976.6 /2000 = 2.05

3.2.3 Model Preparation

A scaled physical model was developed to replicate the tunnel intersection behaviour under controlled laboratory conditions. Plaster of Paris (POP) was selected as the model material due to its ease of availability, workability, and ability to simulate brittle behaviour similar to rock mass [16].

The model dimensions were:

- Length: 425 mm
- Width: 375 mm
- Height: 230 mm

The tunnels were formed using PVC pipes acting as lining material.

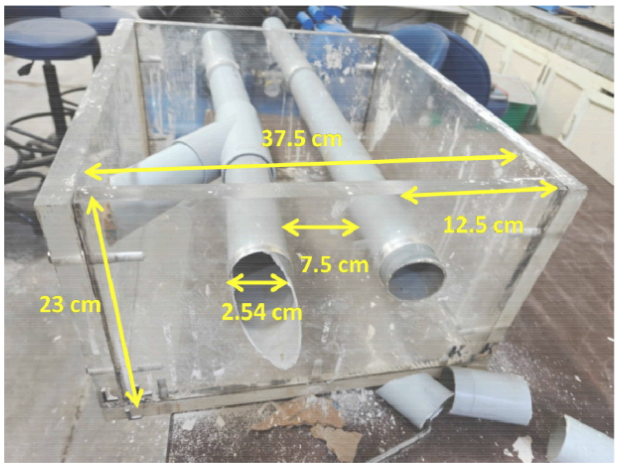

Fig 7. Dimensions of Tunnel intersection laboratory model

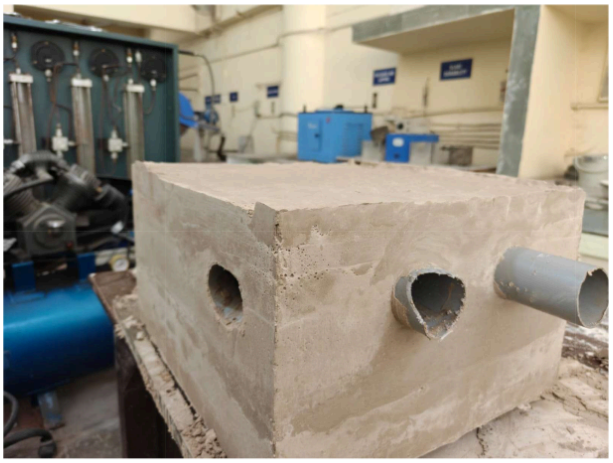
Fig 8. Tunnel model casted in Plaster of Paris

3.2.4 Geometric Configuration

The experimental model was designed to match the numerical setup:

- Tunnel diameter: 5 cm
- Spacing between tunnels: 7.5 cm
- Cover depth: 5 cm
- Intersection angle: 30°
- Distance of intersection from portal: 20 cm

This ensured similarity between numerical and experimental models.

3.2.5 Instrumentation

Instrumentation of the tunnel model was carried out using piezoelectric (PZT) sensors to monitor deformation-induced responses at critical locations of the tunnel system. The experimental setup consisted of four piezoelectric lead zirconate titanate (PZT) patches installed on a Plaster of Paris (POP) tunnel model having overall dimensions of 42.5 cm × 37.5 cm × 23 cm. The sensors were connected to a digital storage oscilloscope for real-time acquisition of voltage signals generated during static loading conditions.

The PZT sensors were selected due to their high sensitivity to stress and deformation variations. When subjected to mechanical deformation, the piezoelectric material generates an electrical charge proportional to the induced strain, which can be measured in the form of voltage output. Thus, the variation in voltage response obtained from the sensors was used to assess the deformation behavior of the tunnel model at different locations.

Four PZT sensors were installed at strategically important locations of the tunnel geometry to capture localized deformation characteristics. Sensor 1 was attached at the portal of the existing tunnel, Sensor 2 at the portal of the escape tunnel, Sensor 3 at the crown region of the tunnel, and Sensor 4 at the intersection zone between the escape tunnel and the newly intersecting tunnel. These locations were selected to evaluate the stress redistribution and deformation response occurring due to tunnel interaction under static loading.

The PZT patches were attached to the surface of the POP tunnel model using adhesive tape to ensure proper contact between the sensor and model surface. The voltage signals generated by the sensors were directly transmitted to a GW Instek GDS-2204A digital storage oscilloscope

having a bandwidth of 200 MHz and sampling capability of 2 GSa/s. The oscilloscope was used to record the voltage-time response obtained from all four sensors during experimentation.

The material and electromechanical properties of the PZT patches used in the present study are summarized in Table X. The dielectric constant of the sensor was 3270, with an electromechanical coupling factor of 0.52. The piezoelectric charge constant and voltage constant were −275 pC/N and -9×10^{-3} Vm/N, respectively. The Young's modulus of the PZT patch was 61 GPa.

The acquired voltage responses from the sensors were analyzed to identify deformation characteristics and relative variations in stress concentration at different tunnel locations during static loading of the model.

Instruments Used:

a) Piezoelectric sensor (Lead ZirconateTitanate)

b) Oscilloscope

c) Probe connecting PZT to Oscilloscope

Fig 9. Instruments used in Monitoring of tunnel behaviour

Table II. Properties of the PZT patch used in the study.

Property	Symbol	Magnitude
Dielectric constant	$\varepsilon_{33}^{T}/\varepsilon_0$	3270
Dielectric loss factor	tanδ	0.016
Electromechanical coupling factor	k_{31}	0.52
Piezoelectric charge constant	d_{31}	−275 pC/N
Piezoelectric voltage constant	g_{31}	-9×10^{-3} Vm/N
Young's modulus	Y	61 GPa

Property	Symbol	Magnitude
Unit weight	γ	7.2 kN/m³

These sensors convert mechanical strain into electrical signals, which were recorded using an oscilloscope.

3.2.6 Loading Procedures

The loading procedure for the tunnel model was carried out using a Compression Testing Machine (CTM) of 2000 kN capacity under controlled laboratory conditions. A static load of approximately 3.9 kN was applied gradually to simulate overburden pressure. The objective of the test was to evaluate the structural response and deformation characteristics of the tunnel model under static vertical loading conditions. The experimental setup consisted of the tunnel specimen, loading frame, CTM, displacement monitoring system, and oscilloscope-based data acquisition system.

The tunnel model specimen of dimensions 42.5 cm × 37.5 cm × 23 cm was prepared and positioned centrally inside the CTM loading frame to ensure uniform load transfer. The tunnel opening was embedded within the model block, and proper alignment was maintained before commencement of loading in order to avoid eccentric loading effects. The model was placed on a rigid base support to simulate stable boundary conditions during testing.

A servo-operated Compression Testing Machine having a maximum loading capacity of 2000 kN was used to apply compressive load on the tunnel model. The load was applied vertically in a gradual and controlled manner so as to simulate static overburden loading conditions acting on underground tunnel structures. The loading was increased incrementally until significant deformation and failure response were observed in the model.

To monitor the deformation behaviour of the tunnel, instrumentation channels were connected at different locations of the specimen. The displacement responses were recorded using PZT sensors connected to a digital oscilloscope. The oscilloscope was utilized for continuous monitoring and recording of signal variations obtained from the sensors during loading. The obtained signals were further used for displacement analysis of different sections of the tunnel model such as crown, sidewall, and invert regions.

During the loading process, the CTM display continuously recorded parameters including applied load, peak load, and corresponding stress values. The peak load observed during testing was approximately 315.8 kN, while the peak stress recorded was approximately 14.03 N/mm². The loading process was continued until noticeable cracking, deformation, and reduction in load carrying capacity occurred in the tunnel model.

Equivalent actual overburden depth calculated through peak stress:

$\sigma_{v=}$14.03 N/mm2

γ=25 kN/m3 (assumed unit weight of rock mass)

Then:

$$H= \sigma_v / \gamma \quad (4)$$

$$H=(14.03\times10^6) / (25\times10^3)$$

$$H\approx561 \text{ m}$$

The tunnel peak stress of 14.03 N/mm^2 simulate the overburden of around 560m.

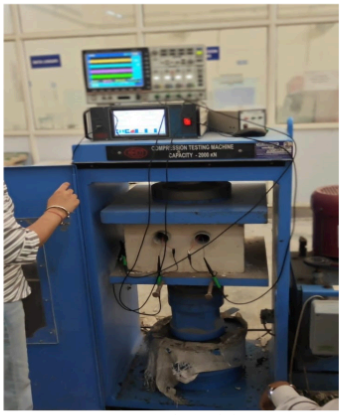

Fig 10. Tunnel model setup

3.2.7 Data Acquisition and Measurement

The deformation response of the tunnel model was captured using PZT sensors connected to an oscilloscope. The electrical signals generated by the sensors were converted into displacement values using calibration relationships as follows [17]:

Voltage- strain relationship:

For PZT Patch : $V = g_{31}\, t\, \sigma$ (5)

Where, V = generated voltage; g_{31} = piezoelectric voltage constant; t = thickness of PZT patch ; σ = stress= E ε

Then: $V = g_{31}\, t\, E\, \varepsilon$ (6)

Thus, $\varepsilon = V / g_{31}\, t\, E$ (7)

Strain-displacement relationship:

Displacement relation: $\delta = \varepsilon\ L$ (8)

δ = displacement; L = effective gauge length/location length

$$\delta = (V\ L) / (g_{31}\, t\, E) \quad (9)$$

Key measurements included:

- Voltage output from sensors (mV)
- Corresponding displacement (μm)
- Variation of deformation at different locations

The recorded data was used for comparison with numerical results.

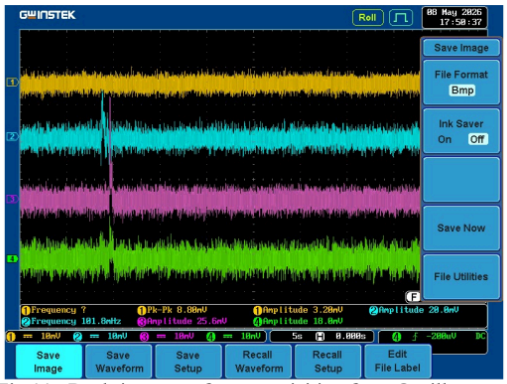

Fig 11. Real time waveform acquisition from Oscilloscope

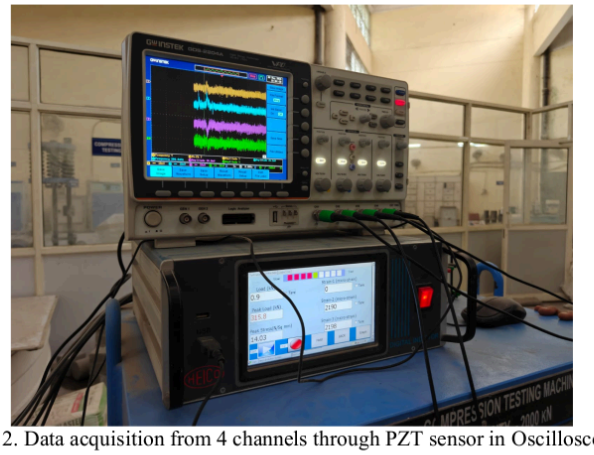
Fig 12. Data acquisition from 4 channels through PZT sensor in Oscilloscope

The acquired voltage signals were further processed to obtain filtered velocity-time response curves for all sensor channels. Signal filtering was performed to remove background noise and improve peak detection accuracy. The processed responses enabled identification of deformation concentration zones and structural behaviour at different tunnel locations under applied loading.

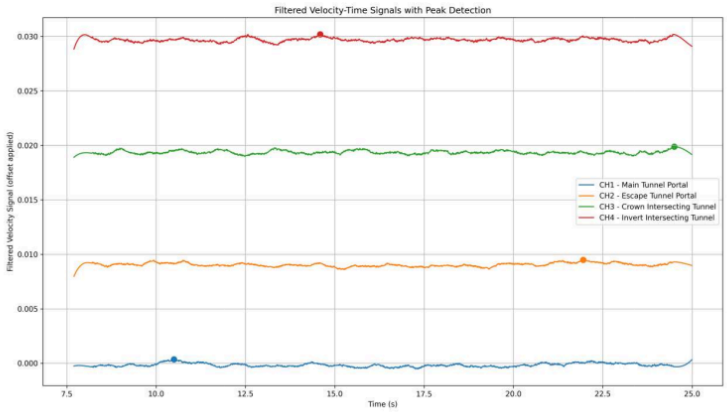

Fig 13. Filtered velocity-time signals obtained from PZT sensor channels with peak detection analysis.

In the present study, smoothing and noise reduction were carried out using the Savitzky–Golay filtering technique. This method smoothens the signal while preserving important waveform characteristics such as peaks, amplitude variations, and transient responses. Unlike ordinary moving average filters, the Savitzky–Golay filter minimizes distortion of significant signal features, making it suitable for structural response monitoring applications [18].

3.3 Validation Methodology:

The validation of numerical results was carried out by comparing them with experimental observations. The following steps were adopted:

1. Extraction of displacement values from 3D Numerical analysis software
2. Conversion of experimental sensor readings into displacement
3. Comparison of deformation at corresponding locations
4. Calculation of percentage variation

This approach ensured the reliability of numerical modelling

3.4 Summary

This study adopts a combined numerical and experimental approach to investigate the deformation behaviour of intersecting tunnels under static loading conditions. The methodology is divided into two major components: (i) three-dimensional numerical modelling using MIDAS GTS NX, and (ii) laboratory-scale experimental modelling using a physical tunnel model instrumented with piezoelectric sensors.

The integration of these approaches enables a comprehensive understanding of deformation characteristics and provides validation of numerical results through experimental observations.

CHAPTER 4. RESULTS AND DISCUSSION

4.1 Numerical Results

The numerical analysis of the tunnel intersection model was carried out to evaluate the deformation characteristics and stress redistribution behaviour under simulated loading conditions. The displacement response of the tunnel system was analysed using contour plots and deformation profiles obtained from the numerical model. Particular emphasis was given to the intersecting region between the main tunnel and the escape tunnel, as this zone experiences stress concentration and structural interaction effects.

The numerical simulation results indicated that displacement concentration predominantly occurred around the intersection region, especially near the crown and invert portions of the tunnel opening. The deformation contours demonstrated progressive displacement variation from the tunnel boundary towards the surrounding medium. The displacement magnitude reduced gradually away from the tunnel opening, indicating stress dissipation within the surrounding material.

The numerical model successfully represented the deformation behaviour of the tunnel system under loading and provided important insight into the critical regions susceptible to excessive deformation and structural instability.

4.1.1 Displacement Contours

The displacement contour plots obtained from the numerical analysis illustrate the deformation distribution around the tunnel openings under applied loading conditions. The contour diagrams indicate higher displacement concentration near the tunnel periphery and intersecting regions due to stress interaction effects between the tunnels.

The contour plots reveal that maximum deformation occurred near the crown and invert portions of the intersecting tunnel section. This behaviour may be attributed to stress concentration developed around the tunnel boundary under simulated overburden loading. The displacement magnitude decreased gradually towards the outer boundary of the model, indicating stable redistribution of stresses into the surrounding medium.

The intersecting tunnel configuration produced localized deformation zones at the junction region, which signifies the influence of tunnel interaction on structural behaviour. The displacement contours further indicate that the intersecting section experiences comparatively higher deformation than the straight tunnel section.

The numerical deformation patterns observed from the contour plots are shown in Figures 12.1 to 12.3.

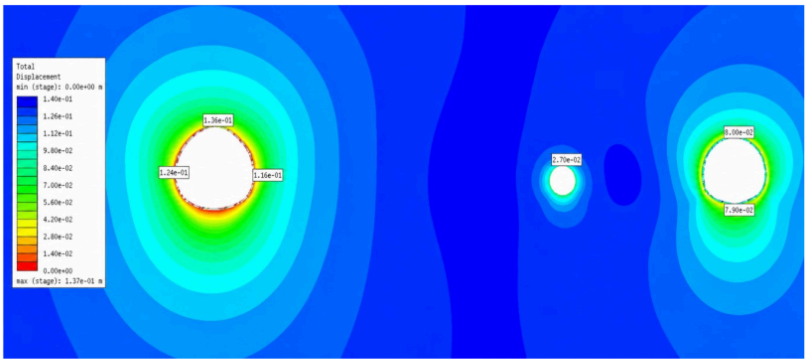

Fig 14.1 . Displacement values at tunnel face

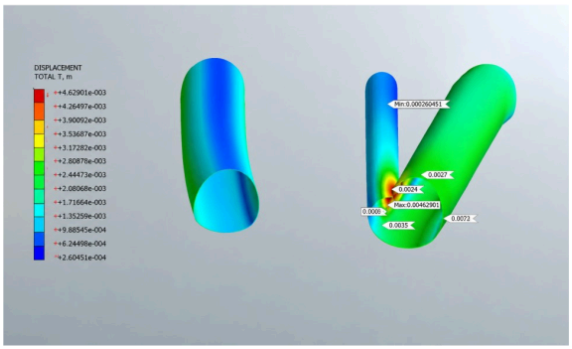

Fig 14.2 . Displacement values at merging section

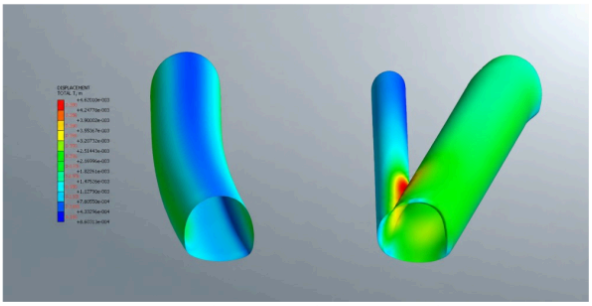

Fig 14.3 . Displacement values at merged section

4.1.2 Displacement Values

Table III. Displacement values at various sections through Numerical Modelling

Location / Region	Approximate Displacement Value
Maximum displacement at intersection region	4.629 x 10^{-3} m
Crown region displacement	3.5 x 10^{-3}m
Invert region displacement	3.0 x 10^{-3} m
Sidewall/intermediate zone	2.4 x 10^{-3} m
Outer tunnel region	1.1 x 10^{-3} m
Minimum displacement zone	2.64 x 10^{-4} m

The displacement values obtained from the numerical model indicated variation in deformation at different locations of the tunnel system. The maximum displacement was observed near the intersecting tunnel region due to localized stress concentration and interaction between the main tunnel and escape tunnel.

The displacement values at the crown and invert regions were found to be comparatively higher than those at the sidewalls and portal sections. This behaviour indicates that vertical compressive loading significantly influences deformation in the upper and lower portions of the tunnel section.

The deformation response further demonstrated that the tunnel intersection acts as a critical zone where stress redistribution leads to increased displacement accumulation. The numerical results

therefore highlight the importance of reinforcement and monitoring at tunnel junction regions during underground construction activities.

4.2 Experimental Results

Experimental investigations were conducted using a 2000 kN Compression Testing Machine (CTM) integrated with PZT-based instrumentation and oscilloscope data acquisition system. The experimental study was performed to evaluate the deformation response of the tunnel model under simulated overburden loading conditions.

The tunnel model specimen was instrumented with four PZT sensors installed at critical tunnel locations including the portal of the main tunnel, portal of the escape tunnel, crown of the intersecting tunnel, and invert of the intersecting tunnel. The sensor outputs were continuously monitored using a multi-channel digital storage oscilloscope during loading.

The experimental observations provided valuable information regarding displacement response, stress concentration zones, and deformation behaviour of the intersecting tunnel system.

4.2.1 Experimental Setup Output

The oscilloscope-based data acquisition system recorded voltage-time signals corresponding to deformation response generated by the PZT sensors during loading. The recorded signals were processed and filtered to remove noise and improve peak identification accuracy.

The filtered velocity-time response curves demonstrated variation in sensor response at different tunnel locations. Among the monitored channels, the crown and invert regions exhibited comparatively higher response amplitudes, indicating significant deformation concentration in the intersecting tunnel section.

Peak detection analysis revealed localized response amplification during loading progression, which may be associated with stress redistribution and crack initiation behaviour within the tunnel model. The response obtained from the tunnel portals was comparatively lower, indicating relatively smaller deformation away from the intersecting region.

The processed oscilloscope output therefore confirmed that the intersecting section of the tunnel experiences the most critical deformation behaviour under applied loading conditions.

Table IV. Voltage-time output of 4 channels recorded through oscilloscope

Channel	Positive Peak Voltage (mV)	Time of Peak (s)	Min Voltage (mV)	Time of peak(s)	Peak-to-Peak (mV)
CH1	4.000	24.630	-5.600	15.87	9.600
CH2	4.400	18.300	-5.600	14.5	10.000
CH3	6.000	8.870	-6.400	16.19	12.400
CH4	4.400	9.080	-7.200	10.72	11.600

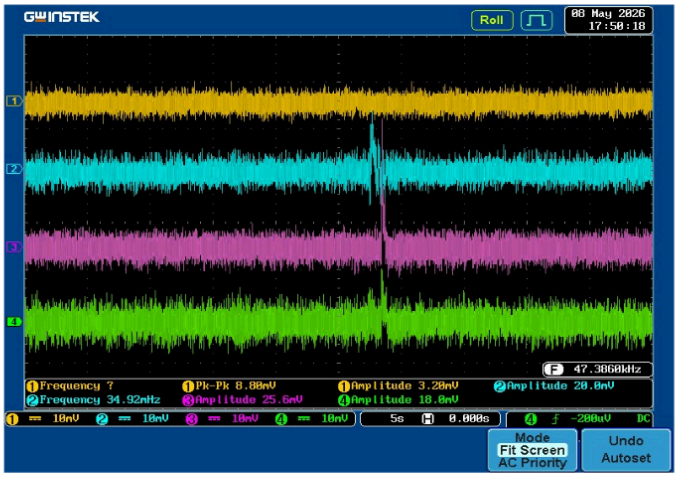

Fig 15. Multi-channel oscilloscope output during tunnel model loading

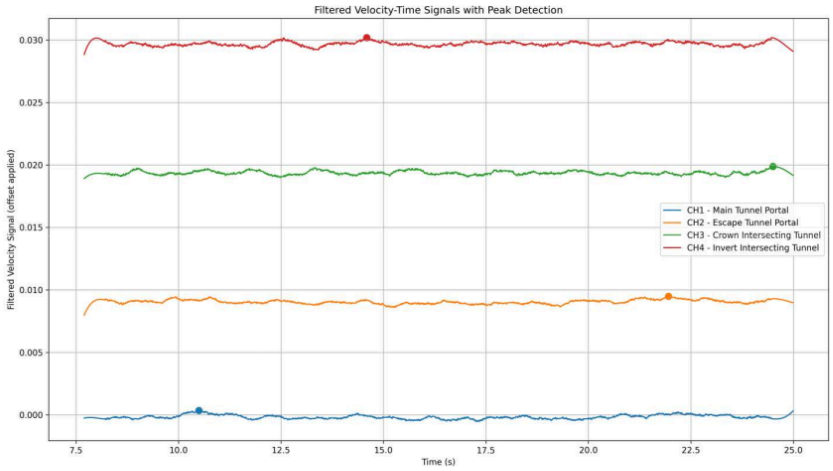

Fig 16. Filtered velocity-time response curves with peak detection.

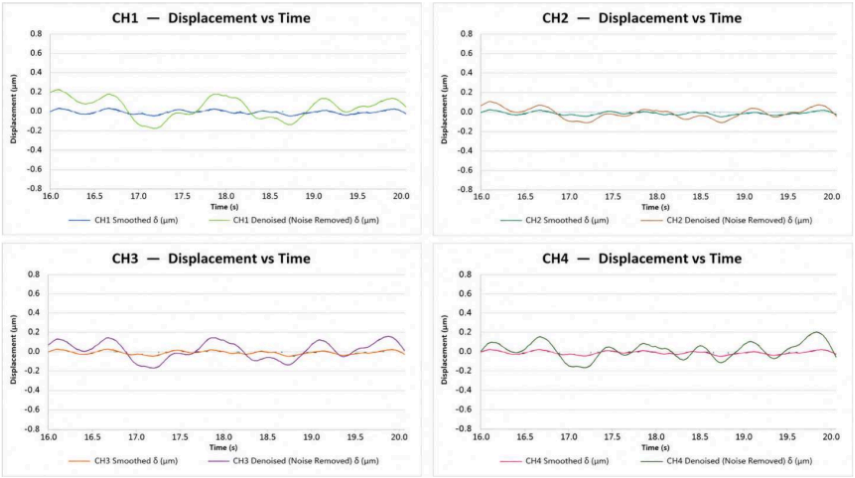

Fig 17. Displacement-time graphs obtained from Velocity-time graphs of 4 channels oscilloscope

4.2.2 Observation

During loading, gradual deformation was observed near the crown and invert regions of the intersecting tunnel section. As the applied load increased, stress concentration developed around the tunnel junction, leading to localized deformation and crack initiation near the critical regions.

The crown region experienced progressive settlement under compressive loading, while the invert region exhibited deformation due to stress redistribution around the tunnel opening. The intersecting tunnel section demonstrated comparatively higher sensitivity to loading when compared with the straight tunnel portions.

The PZT sensor outputs indicated increased voltage response corresponding to deformation progression within the model. Peak signal amplitudes were observed near the critical loading stages, indicating possible initiation of microcracks and structural response concentration.

The experimental observations confirmed that the intersecting tunnel region is structurally more vulnerable under simulated overburden loading conditions.

4.3 Validation

Table V. Numerical and experimental deformation values

Location	Numerical (m)	Experimental (mm)	Variation (%)
Crown	0.0035	1.3115	62.53
Invert	0.0030	1.1658	61.14
Portal A	0.0013	1.0201	21.53
Portal B	0.0028	1.0201	63.57

The larger variations between the numerical analysis and physical modeling results can be attributed to:

- scaling effects in the laboratory model,
- simplified material assumptions in numerical modelling,
- localized PZT sensing response,
- stress transfer limitations,
- and boundary-condition idealization.

Validation of the experimental results was carried out by comparing the deformation behaviour obtained from numerical analysis with the response observed during laboratory testing. The numerical displacement contours showed deformation concentration near the intersecting tunnel region, which was consistent with the experimental observations obtained from PZT sensor monitoring.

Both numerical and experimental results indicated that the crown and invert regions experienced comparatively higher deformation under loading. The response trend observed from the oscilloscope signals also agreed with the displacement concentration zones predicted by the numerical model.

The similarity between numerical contour patterns and experimentally observed deformation behaviour demonstrates the reliability of the adopted numerical modelling and experimental methodology. The validation therefore confirms that the developed tunnel model adequately represents the deformation characteristics of intersecting tunnel systems subjected to simulated overburden loading conditions.

4.4 Discussion of Results

The present study investigated the deformation behaviour of an intersecting tunnel system using both numerical modelling and experimental analysis under simulated overburden loading conditions. The results obtained from displacement contours, laboratory observations, and PZT sensor monitoring demonstrated significant deformation concentration near the tunnel intersection region. The combined investigation provided important insight into the structural response and stability characteristics of intersecting underground tunnel systems.

The numerical analysis revealed that the maximum displacement occurred near the crown and invert regions of the intersecting tunnel section. The displacement contours indicated progressive deformation concentration around the tunnel boundary due to stress redistribution under applied loading. The crown region experienced comparatively higher deformation because of vertical

compressive stress acting directly above the tunnel opening, whereas the invert region exhibited deformation due to stress transfer and redistribution effects within the surrounding medium.

The experimental investigation conducted using the 2000 kN Compression Testing Machine and PZT-based monitoring system showed deformation behaviour similar to the numerical predictions. The voltage-time responses recorded through the oscilloscope indicated higher response amplitudes at the crown and invert locations compared to the tunnel portals. This behaviour confirms that the intersecting tunnel section acts as the most critical zone under overburden loading conditions.

The experimentally measured displacement values were found to be lower than the numerical displacement values. The maximum numerical displacement was observed at the crown region with a value of 3.5mm, whereas the corresponding experimental displacement was 1.31mm. Similarly, the numerical and experimental displacements at the invert region were 3.0 mm and 1.1658 mm respectively. The portal regions exhibited comparatively smaller displacement values in both analyses, indicating reduced deformation away from the tunnel intersection.

CHAPTER 5. CONCLUSIONS AND FUTURE SCOPE

5.1 Conclusion

This chapter presents the key conclusions drawn from the numerical and experimental investigation of deformation behaviour in intersecting tunnels under static loading conditions. The findings are based on a comprehensive analysis carried out using three-dimensional numerical modelling in MIDAS GTS NX and laboratory-scale experimental modelling using a physical tunnel model instrumented with piezoelectric sensors. The chapter also outlines practical recommendations for tunnel design and identifies potential areas for future research.

The study provides significant insights into the deformation behaviour of tunnel intersections. The major findings are summarized as follows:

1. The filtered oscilloscope responses demonstrated identifiable peak signals corresponding to deformation concentration and stress redistribution within the tunnel model. The highest voltage response of 7.2 mV was observed at the crown intersection in physical modeling. Numerical analysis yields deformation value of 3.5 x 10^{-3}m at the crown , confirming that the tunnel junction acts as a localized stress concentration zone under overburden loading.
2. Peak voltage of 6.4 mV corresponding to numerical analysis deformation value of 3.0 x 10^{-3}m was observed at the invert region indicating comparatively higher localized strain concentration near the tunnel intersection.
3. The percentage variation between numerical and experimental displacement values ranged from 20-60%, in which Portal A showed the lowest variation in numerical and physical results.
4. Both Numerical and experimental results identifies crown and invert region as the most critical deformation zones in the intersecting tunnel. Also experimental results do not show any variations in the deformation of portals of main tunnel and intersecting tunnels.

5. Numerical observations demonstrated deformation attenuation away from the tunnel intersection. Portal A exhibited approximately 56.67% lower deformation than the crown region, while Portal B showed approximately 20% lower deformation than the crown region. Experimental observations also demonstrated deformation attenuation away from the intersection, where portal deformation was approximately 22.22% lower than crown deformation.
6. The numerical analysis results shows that deformation at the crown was 16.67% higher than the invert deformation and 25% relative to portal B for the specific case. Similarly, experimental observations indicated that crown deformation increased by approximately 12.50% compared to the invert region and by approximately 28.56% relative to both portal locations.

5.2 Limitations of the Study

While the study provides valuable insights, certain limitations must be acknowledged:

- The experimental model was developed using Plaster of Paris, which may not fully replicate the complex behaviour of natural rock masses, Joints and fracture planes.
- The variation in Numerical analysis and physical modeling results is large.
- The analysis was limited to static loading conditions and does not consider dynamic effects such as seismic loading or blasting.
- Scale effects may influence the accuracy of experimental results.
- The results of numerical modeling and the physical modeling vary by 4-20% which can be minimized by working on the effectiveness of physical model.
- The scaling of overburden was done upto 560m which can be increased and tested for deformation.
- Simplified boundary conditions were used in the numerical model.

5.3 Future Scope

Based on the findings and limitations of the present study, the following recommendations are proposed for future research:

- Investigation of tunnel interaction under dynamic loading conditions, such as earthquakes and blasting
- Study of different intersection angles and spacing configurations
- Use of advanced materials or real rock samples for experimental modelling by creating rock joints and fracture planes
- Field-scale validation of results using actual tunnel projects
- Analysis of excavation sequence on the tunnel behavior at the intersection.
- Effect of excavation of new tunnel intersection on the existing parallel tunnel

Deformation behaviour of intersecting tunnels

ORIGINALITY REPORT

2%	2%	0%	0%
SIMILARITY INDEX	INTERNET SOURCES	PUBLICATIONS	STUDENT PAPERS

PRIMARY SOURCES

1	dspace.dtu.ac.in:8080 Internet Source	2%

Exclude quotes	Off	Exclude matches	< 141 words
Exclude bibliography	Off		

Deformation behaviour of intersecting tunnels

GRADEMARK REPORT

FINAL GRADE

/0

GENERAL COMMENTS

PAGE 1

PAGE 2

PAGE 3

PAGE 4

PAGE 5

PAGE 6

PAGE 7

PAGE 8

PAGE 9

PAGE 10

PAGE 11

PAGE 12

PAGE 13

PAGE 14

PAGE 15

PAGE 16

PAGE 17

PAGE 18

PAGE 19

PAGE 20

PAGE 21

PAGE 22

PAGE 23

PAGE 24

PAGE 25

PAGE 26

PAGE 27

PAGE 28

PAGE 29

PAGE 30

PAGE 31

PAGE 32

PAGE 33

PAGE 34

PAGE 35

PAGE 36